Tenth International Conference on Computational Fluid Dynamics (ICCFD10), Barcelona, Spain, July 9-13, 2018

ICCFD10-056

Aerodynamic Shape Optimization of the Common Research Model based on Improved BFGS Algorithm

Jing Yu*, Jiangtao Huang*, Dong Hao**, and Zhu Zhou*
Corresponding author: haodongcardc@outlook.com (Dong Hao)

* Computational Aerodynamics Institute, China Aerodynamics Research and Development Center, Mianyang, China
** High Speed Aerodynamics Institute, China Aerodynamics Research and Development Center, Mianyang, China

Abstract: Aircraft Aerodynamic Shape Optimization is a complex, large-scale and expensive optimization problem. Adjoint-based gradient optimization method plays a significant role in aerodynamic shape design. In this paper, we mainly focus on the optimization algorithm applied to aircraft aerodynamic design field. BFGS, a quasi-Newton algorithm is employed here, and some improvements in line search and descent direction computation are made to speed up the convergence of the algorithm. After improvements, the physical change of variables in each iteration can be evaluated, set and control. The optimization model with the drag coefficient minimization objective and wing thickness constraints for Wing-Body-Tail Common Research Model (CRM) is established. Aerodynamic shape design for CRM with Wing-Body-Tail Configuration is carried out. The optimization results are compared and discussed. Our optimization procedure reduced the drag from 167.9 counts to 157.2 counts (6.4% reduction) within 11 iterations. The optimization results demonstrate the effectiveness of the improved BFGS method proposed in this paper.

Keywords: Aerodynamic Shape Optimization, BFGS, Optimization Algorithm.

1 Introduction

With the development of the high performance computing, numerical optimization that requires huge computational resources becomes possible, such as Aerodynamic Shape Optimization [1]. In Aerodynamic Shape Optimization process, Computational fluid dynamics (CFD), which is computationally expensive, is repeatedly employed to accurately obtain the flow, providing the objective function value. Furthermore, it should always deal with hundreds of design variables, and the complex constraints in engineering. Aircraft Aerodynamic Shape Optimization is a complex, large-scale and expensive optimization problem. Performing high-fidelity aerodynamic shape optimization is a challenging and expensive task, and the optimization algorithm is one of its key problems.

Generally, the optimization methods could be divided into two classes: gradient-free and gradient-based ones. The former ones are easy to implement and can converge to the global optimum in theory, but their computational cost is much high especially for the large-scale variable problems. The latter ones make use of the gradient information of the objective function, and usually converge to a local optimum. They relatively converge fast and easy to deal with large-scale variables problems. In Aircraft Aerodynamic Shape Optimization, slight local change in wing shape would issue large impact on aerodynamic performance. To finely improve the aerodynamic design, large-scale variables should be taken into account, and gradient-based methods are preferred options for optimization.

From a literature review, much work has been done based on gradient-based method. The aerodynamic shape derivatives are usually computed by adjoint method, which enables the cost of gradient evaluation independent of the number of design variables. Much of these researches focused on adjoint method, and usually applied mature software for optimization, e.g. SNOPT, IPOPT, et al. While some other focused on the aerodynamic performance analysis [2-7]. The Martines' team presented a generalization of the adjoint method in [8]; solved a series of single or multipoint aerodynamic shape optimization problems using multilevel optimization acceleration technique based on the Common Research Model (CRM) wing benchmark case in [9]-[11], as well as Wing-Body-Tail Configuration in [12]-[14]; benchmarked several optimization algorithms, including gradient-based and gradient-free methods in [1], and finally concluded that the gradient-free methods require two to three orders of magnitude more computational effort when compared to the gradient-based; and some other aerodynamic design optimization studies on Blended-Wing-Body Aircraft in [15]. Similar work of other researchers can be found in [16]-[18].

In this paper, we mainly focus on the optimization algorithm. BFGS is employed here, and some improvements in line search and descent direction computation are made to speed up the convergence of the algorithm. The efficiency of the improved BFGS algorithm in CRM Aerodynamic Shape Optimization is discussed.

2 Problem Formulation

2.1 Baseline Geometry

CRM Wing-Body-Tail Configuration is used to be the baseline geometry. The main reference parameters for this baseline configuration are listed in Table 1.

Table 1 Baseline geometry configuration.

Parameters	Value
Reference area	191.8 m^2
Reference chord	6.9 m
Moment reference	(0.0; 0.0; 0.0) m
Reynolds number (Mach = 0.85)	5×10^6

2.2 Mesh Generation

The structured mesh of the CRM Wing-Body-Tail is generated by ANSYS ICEM-CFD software. The mesh we generated for the test case optimization contains 6,620,160 cells (see Figure 1).

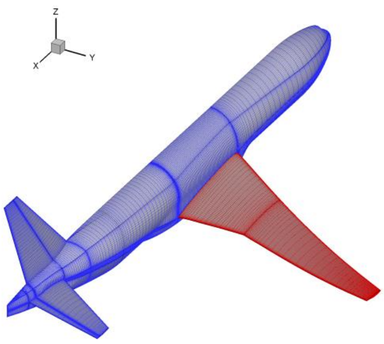

Figure 1: Mesh generation for CRM Wing-Body-Tail

2.3 Design Variables

Free-form deformation (FFD) approach is utilized to parameterize the CRM wing geometry in this paper. Ten airfoil sections are extracted from the CRM wing along with the span-wise direction. The shape of each airfoil is defined by 16 control points, where half of these on the top and the other half on the bottom. So there are 160 design variables in total (see Figure 2).

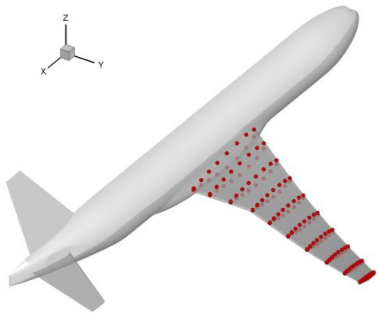

Figure 2: The shape design variables are the z-displacements of 160 FFD control points

2.4 Constraints

(1) Lift constraint: the lift coefficient is set to be 0.5.

(2) Thickness constraint: The relative maximum thickness constraints of three airfoils are taken into account (see Figure 3). One airfoil is located at the wing root; the second one is located at the kink; and the third one it at the wing tip. The original relative maximum thicknesses of these airfoils are 13.69%, 10.52%, and 9.51%, respectively. The relative thickness (Rthick) is calculated by equation (1), where *thickness* represents the actual thickness and *chord* denotes the chord length of the corresponding airfoil.

$$Rthick = thickness / chord \tag{1}$$

In this paper, the relative maximum thicknesses of the three airfoils are constrained to 13.5%, 10.5% and 9.5%, respectively.

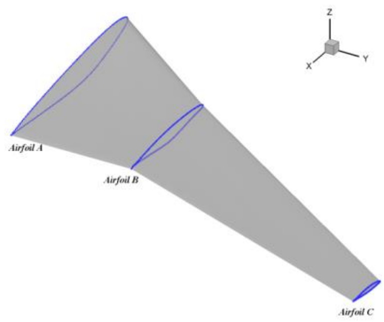

Figure 3: The constrained airfoil sections

2.5 Merit Function

The optimization objective here is to minimize the drag coefficient C_d, as well as satisfying some constraints. The lift constraint could be addressed by CFD solver, in which the attack angle is adjusted and modified to maintain the constant lift coefficient. The thickness constraints are added to the merit function as penalty part (see equation (2)).

$$f(x) = C_d + 0.3 * \sum_{i=A,B,C} (\max(Rthick_i) / Rthick_{ic} - 1)^2 \tag{2}$$

In equation (2), $Rthick_{ic}$ represents the constraint value, i.e. 13.5%, 10.5% and 9.5% corresponding to airfoils A, B, and C, respectively. The penalty coefficient in this paper is set to be 0.3.

2.6 Optimization Model

With the objective of minimizing the drag coefficient of the CRM Wing-Body-Tail geometry in nominal cruising state, the shape design variables are set to be the z-coordinate movements of 160 control points on the FFD volume. All of these points are distributed in ten airfoil sections (see Figure 2). The lift constraint and the maximum thickness constraint of airfoil sections A, B and C (see Figure 3) are taken into account. The complete optimization problem is described in Table 2. (To maintain the lift constraint, the attack angle should also be optimized. The attack angle would be optimized implicitly during Flow Simulation. And this variable would not appear here.)

Table 2 Aerodynamic shape optimization problem.

Function/Variable		Description	Quantity
Minimize	C_d	Drag coefficient	1
With respect to	z	FFD control point z-coordinates	160
		Total design variables	160
Subject to	$C_L = 0.5$	lift constraint	1
$\max(Rthick_A) = 13.5\%$		Maximum thickness constraint of airfoil section 1	1
$\max(Rthick_B) = 10.5\%$		Maximum thickness constraint of airfoil section 2	1
$\max(Rthick_C) = 9.5\%$		Maximum thickness constraint of airfoil section 3	1
		Total constraints	4

3 Methodology

3.1 The Main Framework

The main framework used for aerodynamic shape optimization in this paper is illustrated in Figure 4. There are five key numerical tools and methods that are used for shape optimization, i.e. Geometry Parameterization, Mesh Perturbation, CFD solver for Flow Simulation, Gradient Solver, and Optimizer.

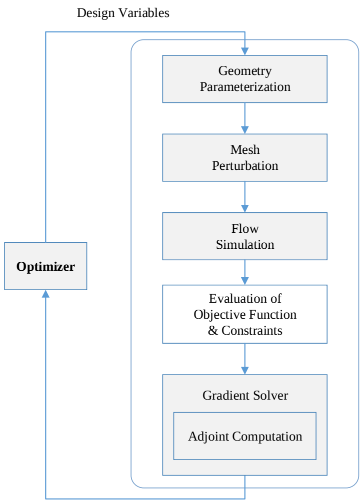

Figure 4: The main framework for aerodynamic shape optimization

The free-form deformation (FFD) approach is employed for Geometric Parametrization, which parametrizes the geometry changes rather than the geometry itself. Mesh Perturbation is carried out by a mesh deformation technique, modifying the displacements of the whole grid points under the basis of the radial basis functions. In Flow Simulation, a self-developed CFD solver PMB3D with a Reynolds-averaged Navier-Stokes (RANS) model is put into use. PMB3D is a large-scale parallel structured grid RANS solver. In Gradient Solver, another self-developed, parallelized adjoint equation solver, Adjoint3D is employed for gradient computation. In Optimizer, the gradient-based algorithm BFGS is employed and improved.

3.2 The Improved BFGS algorithm

Figure 5 shows the main optimization process of BFGS. D_k is the descent direction, $alpha$ is the step length of the line search. Different from the conventional BFGS algorithm, the descent direction would be normalized before line search. The initial $alpha$ is obtained by users according to the optimization experience. And the interpolation method is employed to update $alpha$, speeding up the convergence of the iteration.

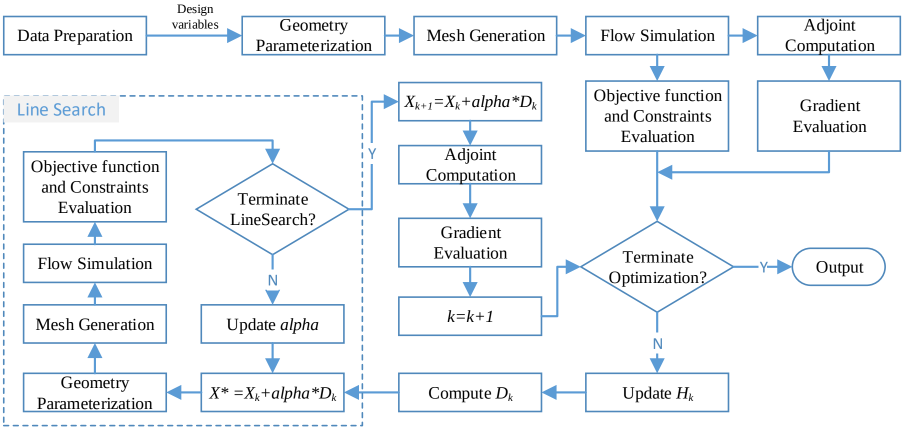

Figure 5: The main framework of optimization process.

The detailed steps of BFGS algorithm is as follows.

Step 0: Give the initial guess x_0 and the initial symmetric positive definite matrix H_0, and let $k = 0$. Compute the gradient vector $g_k = \nabla f(x_0)$.

Step 1: Check if the terminate conditions are satisfied or not. If yes, go to step 6.

Step 2: Calculate the descent direction D_k.

$$D_k = -H_k g_k \tag{3}$$

$$s_k = x_{k+1} - x_x \tag{4}$$

$$y_k = g_{k+1} - g_k \tag{5}$$

$$H_{k+1} = \begin{cases} H_k & \text{if } s_k^T y_k \le 0 \\ H_k - \dfrac{H_k y_k y_k^T H_k}{y_k^T H_k y_k} + \dfrac{s_k s_k^T}{s_k^T y_k} & \text{if } s_k^T y_k > 0 \end{cases} \tag{6}$$

Step 3: Line search and find one proper step length $alpha$ satisfy equation (7).

$$f(x_k + \alpha_k \bar{D}_k) - f(x_k) \le 0 \tag{7}$$

Step 4: Let $x_{k+1} = x_k + \alpha_k \bar{D}_k$. Compute $g_{k+1} = \nabla f(x_{k+1})$.

Step 5: Let $k = k+1$, and then go to step 1.

Step 6: End, and x_k is the approximate minimum point.

Line search, also called one-dimensional search, is a local search in the BFGS framework, aiming at finding one step length to satisfy the descending condition equation (7). Lots of line search methods have been proposed [19], such as golden section search, interpolation, Wolfe principle, and Armijo principle etc. No matter what method is put into use, the key problem in practice is to define the initial step length. A good initial step length could sharply decrease the local iteration, speeding up the convergence of the whole algorithm. In addition, due to the expensive computation cost in CFD, in the application of aircraft aerodynamic design, we need minimum number of calls to CFD solver and the gradient solver. In this paper, quadratic interpolation is employed to search the step length. In order to define a reasonable initial guess of the step length, we normalize the descent direction D_k first, and then define an initial guess by engineering experience. When D_k is normalized, the maximum number in $\bar{D}_k$ vector is 1. And the step length then represents the maximum change in the variables, i.e. the step length has a physical meaning.

4 Simulation and Discussion

The optimization results with lift and thickness constraints for the CRM Wing-Body-Tail aircraft aerodynamic design under the nominal flight condition (Mach 0.85, Re = 5.0e6) are presented in this section. The grid of 6,620,160 cells is used for the optimization. Based on the FFD method, 160 design variables described in Figure 2 are optimized. The initial step length is 0.01, which means that the maximum change of the aircraft shape during the optimization process is 1 cm. Our optimization procedure reduced the drag from 167.9 counts to 157.2 counts (6.4% reduction) within 11 iterations. The comparisons between the initial model and the optimization results are illustrated in Figure 6. The comparison of the airfoil sections are given in Figure 7. The iteration process is depicted in Figure 9. The constraints variation is described in Figure 8. The number of objective evaluation and the corresponding merit function value and drag coefficient value are described in Figure 10.

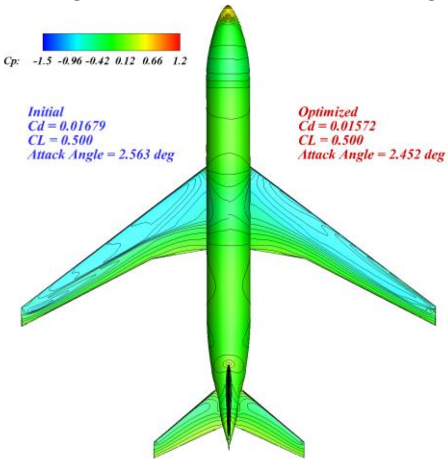

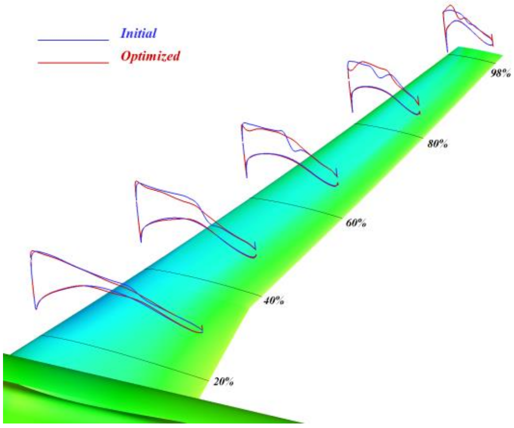

Figure 6: Comparison of the optimization results with the baseline configuration.

It can be seen from Figure 6 there are closely spaced pressure contour lines exhibited in the baseline wing, spanning a significant portion of the wing. And the intensive pressure contour lines indicate a shock. While in the optimized wing, the pressure contour lines are near uniform spacing, indicating shock elimination under the nominal flight condition. The airfoil Cp distributions of different position (as % of range) are also depicted in Figure 6. After optimization, the sharp increase in local pressure due to the shock becomes a gradual change from the leading edge to the trailing edge, indicating a shock-free state.

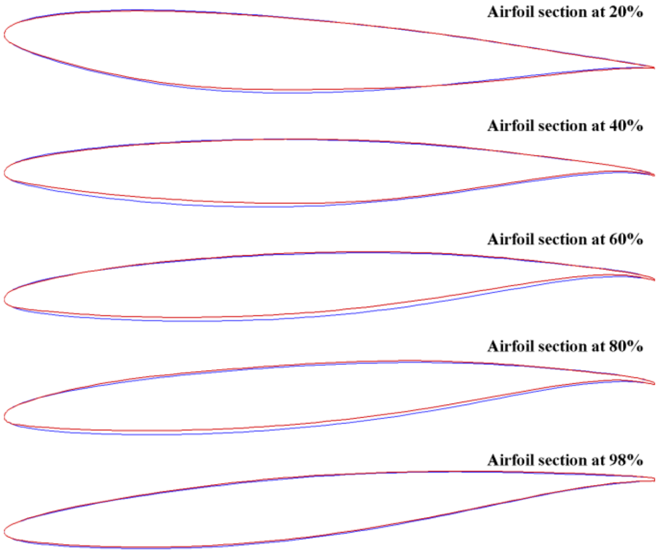

Figure 7: Comparison of the airfoil sections.

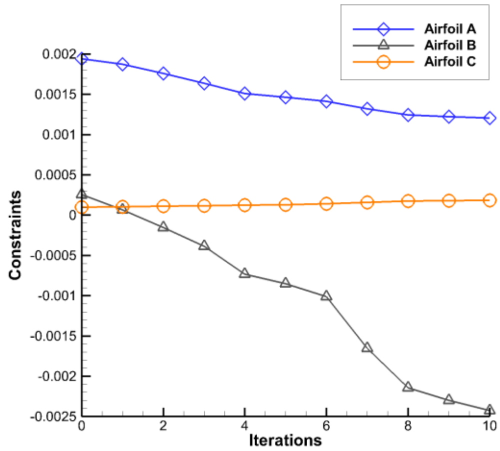

Figure 8: Constraints variation.

It can be seen from Figure 7 the thickness change of the airfoil sections before and after optimization is not significant. This is due to that the airfoil thicknesses are constrained to constant values, which are near to their initial thickness values. But it still can be seen, most of the airfoils in Figure 7 are slightly thinner than the original ones. Figure 8 illustrates the constraints change with the optimization process. The constraint value is calculated as: $Rthick_i - Rthick_{ic}$, where $i = A, B, C$. It can be seen from Figure 8, the relative maximum thickness of airfoils A and B decreases while that of airfoil C becomes slightly larger. The change of airfoil B is more obvious than others.

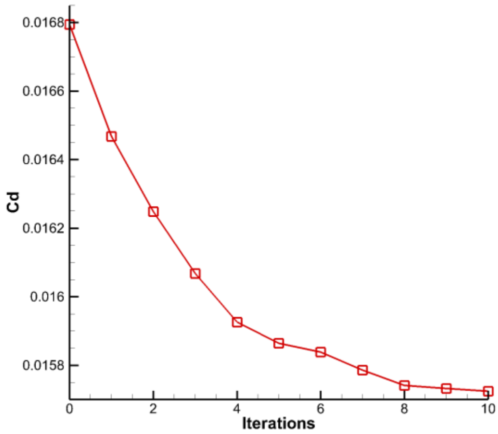

Figure 9: Iteration process.

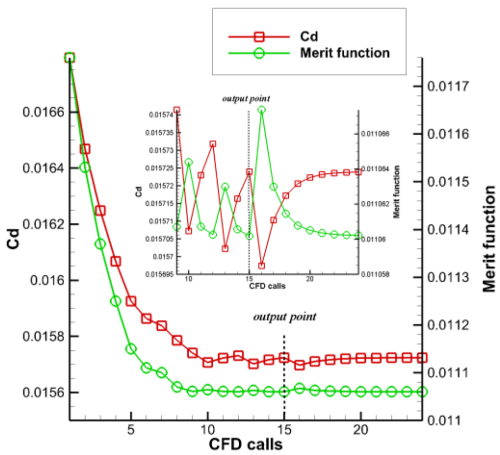

Figure 10: Number of objective evaluation vs. the merit function value and the drag coefficient.

Figures 9 and 10 separately describe the drag coefficient and the merit function change with the iteration process and the CFD solver calls. It can be seen from Figure 9 the whole optimizing process converged within 11 iterations. The optimal solution is obtained at iteration 10, and at iteration 11 the optimizer can not found a better solution in line search. The whole optimization is terminated by the failure of line search.

For each objective evaluation, the CFD solver should be called once. At the beginning of the optimization (before iteration 9), the line search could always find a superior point at the first search. At iterations 9 and 10, the line search searches three times to obtain a superior point, while at iteration 11 the line search tries 9 times, and then terminate the optimization as the step length is too small to continue.

Seeing the partial enlarged drawing in Figure 10, some points with smaller drag coefficient are evaluated, but due to the penalty on constraints, the corresponding merit function values are relative high and these points are abandoned.

The simulation results demonstrate the effectiveness of the improved BFGS algorithm and the optimization strategy to certain degree. In terms of the algorithm efficiency, the improved BFGS algorithm work well. 6.4% reduction of drag coefficient has been obtained by only ten iterations and 15 CFD solver calls. The initial step length in line search can easily be determined by introducing engineering experience, as the step length represents the design variable variation range in physics. A good initial step length could efficiently prevent meaningless searching, and speed up the convergence velocity. In terms of the optimization results, the optimized shape indicates shock elimination. Compared with some other gradient-based algorithm, such as SQP (Sequential Quadratic Programming), BFGS is not good at dealing with constraints. On accounting of equality or un-equality constraints, SQP algorithm may be more proper. However, the effectiveness of the improvements in line search could be demonstrated in this paper. And it also could be introduced to the other gradient-based algorithms.

5 Conclusions

Performing high-fidelity aerodynamic shape optimization is a challenging and expensive task, and the optimization algorithm is one of its key problems. Adjoint-based gradient optimization method plays a significant role in aerodynamic shape design. In this paper, we mainly focus on the optimization algorithm applied to aircraft aerodynamic design field. BFGS, a quasi-Newton algorithm is employed here, and some improvements in line search and descent direction computation are made to speed up the convergence of the algorithm. After improvements, the physical change of variables in each iteration can be evaluated, set and control. The optimization model with the drag coefficient minimization objective and wing thickness constraints for Wing-Body-Tail Common Research Model (CRM) is established. Aerodynamic shape design for CRM with Wing-Body-Tail Configuration is carried out, and the optimized shape indicates shock elimination. The simulation results demonstrate the effectiveness of the improved BFGS algorithm and the optimization strategy to certain degree. Compared with some other gradient-based algorithm, such as SQP, BFGS is not good at dealing with constraints. In our near future, the proved improvements in line search would be introduced to SQP, improving the optimization algorithm in dealing with constraints in aerodynamic shape design.

Acknowledgement

This work was supported by National Key R & D Program of China under Grant No. 2016YFB0200704, Equipment Advance Research Project of China under Grant No. 41406030301, and the National Natural Science Foundation of China under Grant No. 71601179.

References

[1] Z. Lyu, Z. Xu, and J.R.R.A. Martins, Benchmarking Optimization Algorithms for Wing Aerodynamic Design Optimization, in The Eighth International Conference on Computational Fluid Dynamics (ICCFD8), Chengdu, Sichuan, China, July 14–18, 2014.

[2] Reuther, J. J., Jameson, A., Alonso, J. J., Rimlinger, M. J., and Saunders, D., Constrained Multipoint Aerodynamic Shape Optimization Using an Adjoint Formulation and Parallel Computers, Part 1, Journal of Aircraft, Vol. 36, No. 1, 1999, pp. 51-60. doi:10.2514/2.2413.

[3] Reuther, J. J., Jameson, A., Alonso, J. J., Rimlinger, M. J., and Saunders, D., Constrained Multipoint Aerodynamic Shape Optimization Using an Adjoint Formulation and Parallel Computers, Part 2, Journal of Aircraft, Vol. 36, No. 1, 1999, pp. 61-74. doi:10.2514/2.2414.

[4] Hicken, J. E. and Zingg, D. W., Aerodynamic Optimization Algorithm with Integrated Geometry Parameterization and Mesh Movement, AIAA Journal, Vol. 48, No. 2, 2010, pp. 400-413. doi:10.2514/1.44033.

[5] Hicken, J. E. and Zingg, D. W., Induced-Drag Minimization of Nonplanar Geometries Based on the Euler Equations, AIAA Journal, Vol. 48, No. 11, 2010, pp. 2564-2575. doi:10.2514/1.J050379.

[6] Lyu, Z., Kenway, G., Paige, C., and Martins, J. R. R. A., Automatic Differentiation Adjoint of the Reynolds-Averaged Navier-Stokes Equations with a Turbulence Model, 43rd AIAA Fluid Dynamics Conference and Exhibit, June 2013.

[7] Jameson, A., Martinelli, L., and Pierce, N., Optimum Aerodynamic Design using the Navier-Stokes Equations, Theoretical and Computational Fluid Dynamics, Vol. 10, No. 1-4, 1998, pp. 213-237. doi:10.1007/s001620050060

[8] Martins, J. R. R. A. and Hwang, J. T., Review and Unification of Methods for Computing Derivatives of Multidisciplinary Computational Models, AIAA Journal, Vol. 51, No. 11, 2013, pp. 2582-2599. doi:10.2514/1.J052184.

[9] Liem, R.P., J.R.R.A. Martins, and G.K.W. Kenway, Expected Drag Minimization for Aerodynamic Design Optimization Based on Aircraft Operational Data. Aerospace Science and Technology, 2017.

[10] G.K.W. Kenway, and J. R. R. A. Martins, Multipoint Aerodynamic Shape Optimization Investigations of the Common Research Model Wing. AIAA JOURNAL, 2016. 54(1): p. 113-128.

[11] Zhoujie Lyu and J. R. R. A. Martins. Aerodynamic Shape Optimization Investigations of the Common Research Model Wing Benchmark. AIAA Journal, 2014

[12] S. Chen, Z. Lyu, G. K. W. Kenway, and J. R. R. A. Martins. Aerodynamic shape optimization of the Common Research Model wing-body-tail configuration. Journal of Aircraft, 2015. doi:10.2514/1.C033328

[13] G. K. W. Kenway and J. R. R. A. Martins. Aerodynamic shape optimization of the CRM configuration including buffet-onset conditions. In 54th AIAA Aerospace Sciences Meeting. American Institute of Aeronautics and Astronautics, January 2016. doi:10.2514/6.2016-1294

[14] Martins, J.R.A., Wing design via numerical optimization. SIAG/OPT Views and News, 2015. 23(1): p. 2-7.

[15] Zhoujie Lyu and J. R. R. A. Martins. Aerodynamic design optimization studies of a blended-wing-body aircraft. Journal of Aircraft. doi:10.2514/1.C032491

[16] Anderson, M.B., J.E. Burkhalter, and R.M. Jenkins, Missile Aerodynamic Shape Optimization Using Genetic Algorithms. Journal of Spacecraft and Rockets, 2000. 37(5): p. 663-669.

[17] Tang, Z., J. Périaux, and J. Dong, Constraints handling in Nash/Adjoint optimization methods for multi-objective aerodynamic design. Comput. Methods Appl. Mech. Engrg., 2014. 271: p. 130-143.

[18] Wang Long, Song Wenping, and Yang Xudong, A New and Effective Method of Multi-Objective Drag Reduction with Fixed Angle of Attack Based on Adjoint Equation (in Chinese). Journal of Northwestern Polytechnical University, 2012. 30(1): 68-72.

[19] Jorge Nocedal, and Stephen J. Wright, Numerical Optimization. Springer Science and Business Media Inc., 2006.